International Journal of Earth, Energy and Environmental Sciences
ISSN: 2517-942X
Vol:9, No:5, 2015

First-Principles Investigation of the Structural and Electronic Properties of $Mg_{1-x}Bi_xO$

G. P. Abdel Rahim, M. María Guadalupe Moreno Armenta, Jairo Arbey Rodriguez

***Abstract*—**We investigated the structure and electronic properties of the compound $Mg_{1-x}Bi_xO$ with varying concentrations of 0, ¼, ½, and ¾ *x* bismuth in the the cesium chloride (CsCl), zinc-blende (ZnS), nickel arsenide (NiAs) NaCl (rock-salt) and WZ (wurtzite) phases. We calculated. The calculations were performed using the first-principles pseudo-potential method within the framework of spin density functional theory (DFT).

***Keywords*—**DFT, $Mg_{1-x}Bi_xO$, pseudo-potential, rock-salt and wurtzite.

I. Introduction

MAGNESIUM oxide (MgO) and its alloys have been studied extensively, both theoretically and experimentally, because of its electronic, magnetic, and thermodynamic properties. G. Patricia Abdel Rahim et al. found that increasing the Bi concentration in $Mg_{1-x}Bi_xO$ in the NaCl phase produces an increase in the lattice constant and energy but a decrease the bulk modulus [1]. Whilst Amroni et al. found that increasing the Zn concentration in $Mg_xZn_{1-x}O$ in the NaCl phase produces a decrease in the lattice constant and the bulk modulus but increases the energy gap and the effective mass [2]. G. Murtaza et al. found that this material would be useful in optoelectronic devices working in ultra violet [3]. G. Zhao concluded that the research of the properties of the perovskite $MgSiO_3$ enables us to achieve a deeper understanding of the origin and evolution of planets [4]. On the other hand, bismuth (Bi) is a quasi-two-dimensional metal with peculiar spin properties. Its possible application as a spin source or a spin filter enables Bi to be used in both spintronics and quantum computing [5].

As is known, Bi is stable in the rhombohedral phase [5], [6] and MgO is stable in the cubic phase [7] were carried out in the cubic and hexagonal phases and this research is mainly based on studying the structural stability of $Mg_{1-x}Bi_xO$ compound at various concentrations. In order to achieve the objective of this research, we carried out calculations on the NaCl (rock-salt) and WZ (wurtzite) phases. The calculations were performed in the phase NaCl and WZ because previous calculations obtained by us in the phases (NaCl), cesium chloride (CsCl), zinc-blende (ZnS), nickel arsenidine (NiAs) and wurtzite (WZ); we obtained that the ground state the compound $Mg_{1-x}Bi_xO$ is in the phases NaCl and WZ. The concentrations used were 0, ¼, ½, and ¾ *x* for each phase. To study the stability, plots of energy as a function of volume were made for each phase and each *x*. From these plots, the phase for the ground state is found for each *x*, additionally, it is possible to determine if there is a phase transition induced by pressure. All of this is with the aim of exploring the chemical-physical properties that the combination of a semimetallic material (Bi) and a semiconductor one (MgO) could have.

G.P Abdel Rahim is with the Universidad Antonio Nariño, by means of project title "Propiedades físicas de la adsorción de bismuto sobre la superficie/ (001) cubica-MgO en un slab 2x2, number 20141086 de la UAN". Project number 20141086 in Colombia, (phone: +57 (1) 3152980, e-mail: gabdelrahim@uan.edu.co).

M. María Guadalupe Moreno Armenta is with the Universidad Nacional Autónoma de México, UNAM by means of DGAPA project, IN102714-3. Calculations were performed at the Dirección General de Cómputo y de Tecnologías de la Información y Comunicación de la Universidad Nacional Autónoma de México (DGCTIC-UNAM) supercomputing center proyect SC14-1-I-2. (e-mail: aeoaun25@gmail.com).

Jairo Arbey Rodriguez is with the Universidad Nacional de Colombia, Bogotá, cluster of Grupo de Estudio de Materiales GEMA, of Dept. of Physics (e-mail: jairoarbey@gmail.com).

II. Method

Calculations were performed using the first-principles pseudo-potential method in the framework of the spin density-functional theory (DFT) by means of Quantum Espresso Code [8]. Exchange and correlation effects were dealt with using the generalized gradient approximation (GGA) implemented in the Perdew–Burke–Ernzerhof functional (PBE) [9]. Ultrasoft pseudo-potentials were employed [10]. The wave function was expanded in plane waves up to a cutoff of 40Ry. A gamma-centered Monkhorst–Pack [11] *k*-point grid of 4×4×2 for hexagonal cases and 4×4×4 for cubic cases was used in the First Brillouin zone. The Methfessel–Paxton smearing technique with a smearing width of 0.272 eV was adopted [12]. The convergence for the energy was 0.0001Ry. For determining the *x* value, a supercell model was implemented. For example, in wurtzite a 1×1×2 supercell was used, and a $\sqrt{2}$ $\times\sqrt{2}$ $\times 2$ supercell was used in the simple cubic phase.

III. Structural Properties

Figs. 1-4 show the energy of the compound versus volume (E vs V) by unit formula of $Mg_{1-x}Bi_xO$. It can be observed that each curve has minimum energy, which indicates that the phase is metastable. On the basis of the figures MgO and 25% the Bi, it is possible to conclude that the ground state is the rock-salt phase. But for 75% the Bi ground state is the WZ phase.

Fig. 5 shows the cohesion energy as a function of the Bi concentration in $Mg_{1-x}Bi_xO$ for the NaCl and WZ structures. It is possible to conclude what is set forth in the previous paragraph and also that for concentrations minor the ~61% of Bi, the most stable structure is NaCl, for higher values than

~67% the most stable structure is WZ and for concentrations between ~61% to ~67% both structures can coexist.

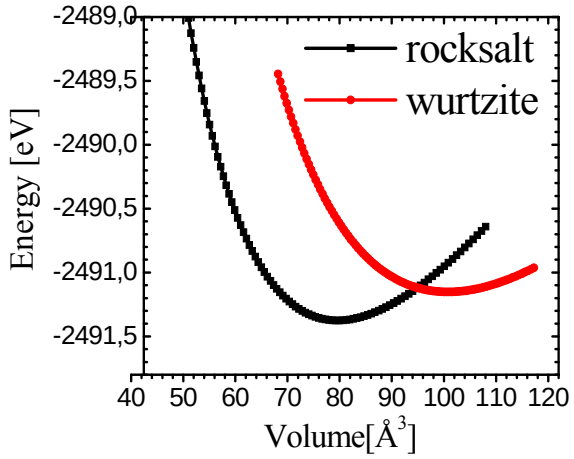

Fig. 1 Energy vs. volume for the MgO compound in two structures

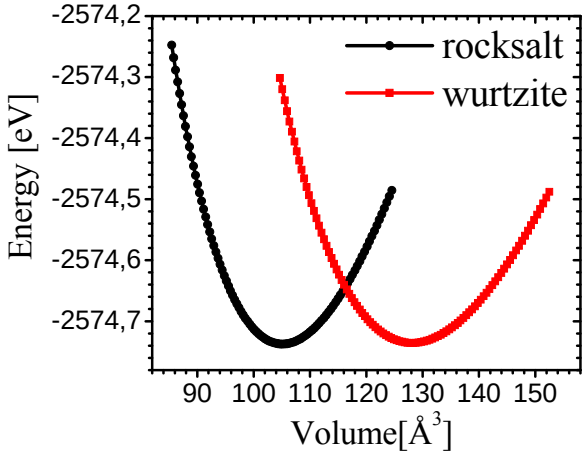

Fig. 2 Energy vs. volume for the $Mg_{0.75}Bi_{0.25}O$ compound in two structures

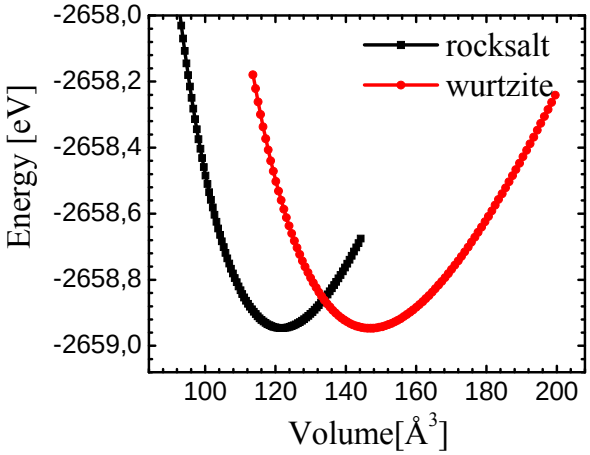

Fig. 3 Energy vs. volume for the $Mg_{0.50}Bi_{0.50}O$ compound in two structures

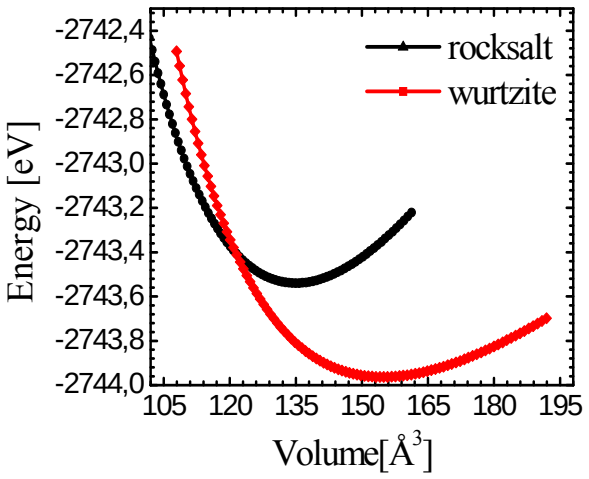

Fig. 4 Energy vs. volume for the $Mg_{0.25}Bi_{0.75}O$ compound in two structures

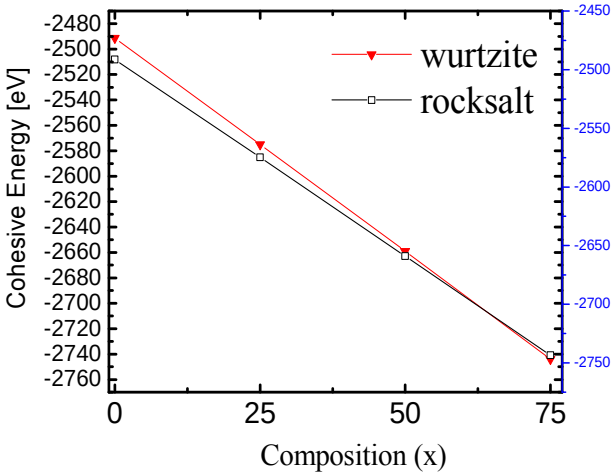

Fig 5 Cohesive energy vs concentration of Bi

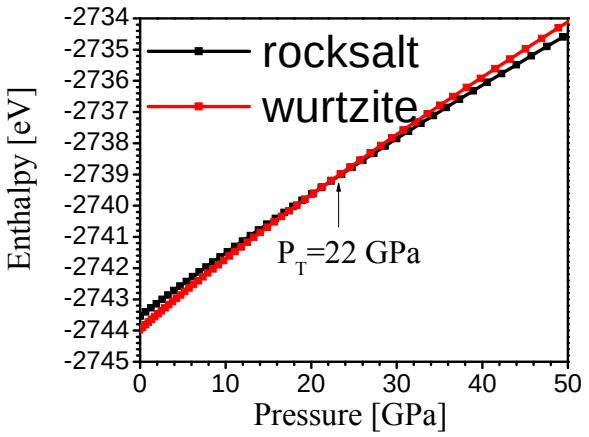

Fig. 6 Enthalpy vs. pressure

Fig. 6 notes enthalpy versus pressure for value ¾ *x* Bi and show an intersection between the phases WZ and NaCl at P_T ~ 22 GPa with a volume of reduction of 6% from ~ 122Å^3 to ~

115Å^3. When making the graphic the enthalpy versus pressure for values 0, ¼ and ½ *x* bismuth, it was found that the curves for both phases are not crossed for values positive pressure, this tells us that is not possible to occur a phase transition.

Tables I and II report the structural parameters obtained. These parameters are determined by fitting the curves of E vs. V to Murnaghan's state equation [13]. In the tables, c/a is the relationship between lattice parameters, *V* is the volume of the unitary cell, *B* is the bulk modulus, and E_0 is the cohesion energy.

TABLE I
THE STRUCTURAL PARAMETERS OF $MG_{1-X}BI_XO$ IN THE ROCK-SALT STRUCTURE

	MgO	$Mg_{0,75}Bi_{0,25}O$	$Mg_{0,5}Bi_{0,5}O$	$Mg_{0,25}Bi_{0,75}O$
a_0(Å)	3.038	3.337	3.504	3.627
c/a	2.828	2.828	2.828	2.828
V (Å^3)	79.61	105.11	121.72	135.00
B (GPa)	142.80	118.82	109.90	106.06
E_o (eV/cell)	-2491.36	-2574.73	-2658.94	-2743.53

TABLE II
THE STRUCTURAL PARAMETERS OF $MG_{1-X}BI_XO$ IN THE WURTZITE STRUCTURE

	MgO	$Mg_{0,75}Bi_{0,25}O$	$Mg_{0,5}Bi_{0,5}O$	$Mg_{0,25}Bi_{0,75}O$
a_0(Å)	3.302	3.577	3.749	3,852
c/a	3.230	3.240	3.261	3,092
V (Å^3)	100.78	128.14	148.19	261.78
B (GPa)	109.60	94.11	83.62	62,68
E_o (eV/cell)	-2491.15	-2574.73	-2658.94	-2743,96

Fig. 7 shows the lattice parameter (*a*) as a function of *x*. It can be seen that *a* increases with *x* from Bi, almost following Vegard's law, which can be explained because of the atomic radius of Bi. Fig. 8 shows the behavior of the bulk modulus (B) as a function of *x*. The tendency of B decreases with *x*, which indicates that the material becomes less rigid. This feature is possibly due to the 6*p* electrons of Bi, 2*p* of O and 3*s* of Mg forming increasingly stronger hybridizations when the Mg increases.

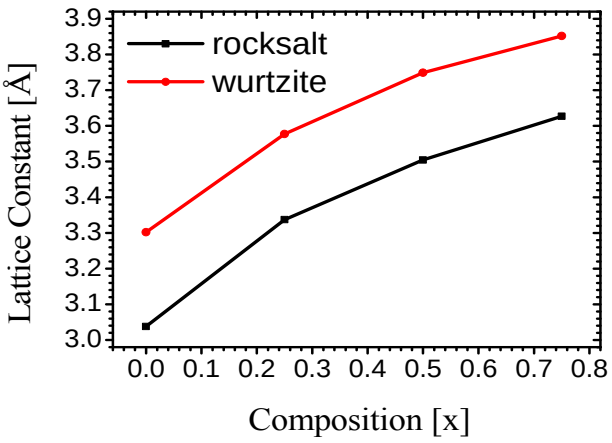

Fig. 7 Lattice constant vs concentration of Bi

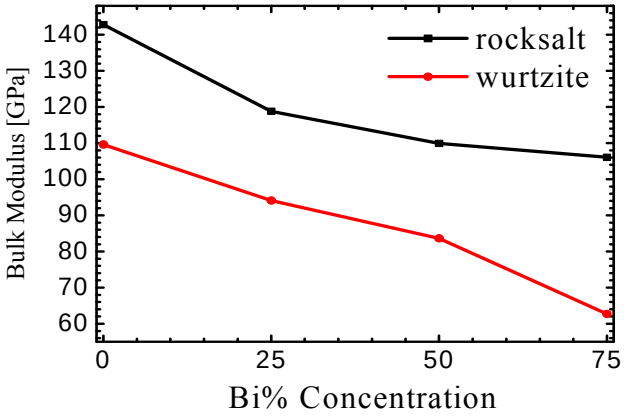

Fig. 8 Bulk Modulus vs Concentration of Bi

IV. ELECTRONIC PROPERTIES

In this section we study the density of states (DOS) and the band structure for concentrations of 0, ¼, ½, and ¾ *x* of bismuth in the NaCl and WZ phases. The study was conducted in these phases due to a previous study we did on the structural properties of the $Mg_{1-x}Bi_xO$ compound. It was found that this compound is stable or metastable, at least in these structures.

Figs. 9-16 show the band structure, where the vertical axis corresponds to the energy in eV and the horizontal axis corresponds to the number of *k* waves along some directions of high symmetry in the first Brillouin zone (PZB). The zero energy is placed at the Fermi level (NF). Below the NF the valence bands are found, and above are the conduction bands. Computations were performed at P = 0.

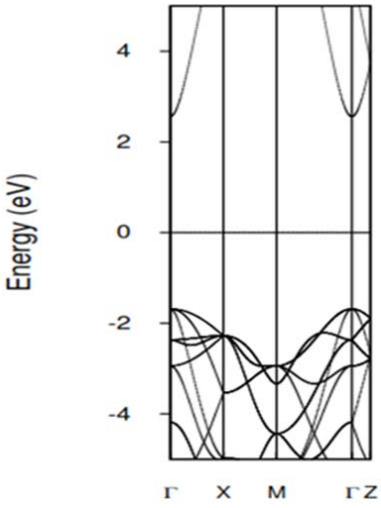

Fig. 9 Bands of NaCl in MgO

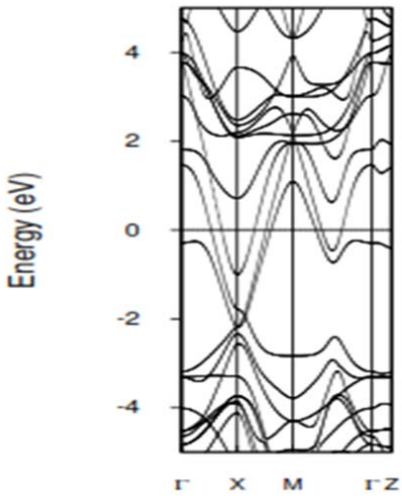

Fig. 10 Bands of NaCl in $Mg_{0.75}Bi_{0.25}O$

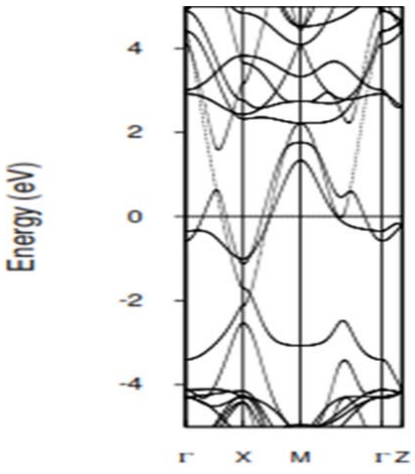

Fig. 11 Bands of NaCl in $Mg_{0.5}Bi_{0.5}O$

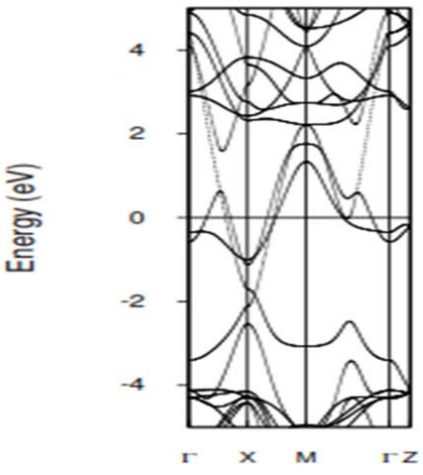

Fig. 12 Bands of NaCl in $Mg_{0.25}Bi_{0.75}O$

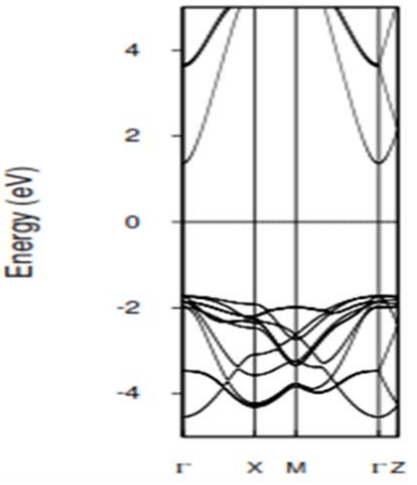

Fig. 13 Bands of WZ in MgO

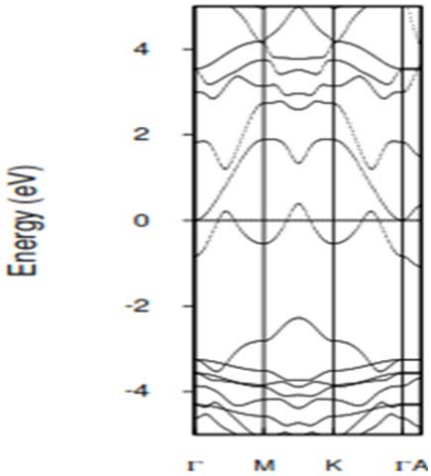

Fig. 14 Bands of WZ in $Mg_{0.75}Bi_{0.25}O$

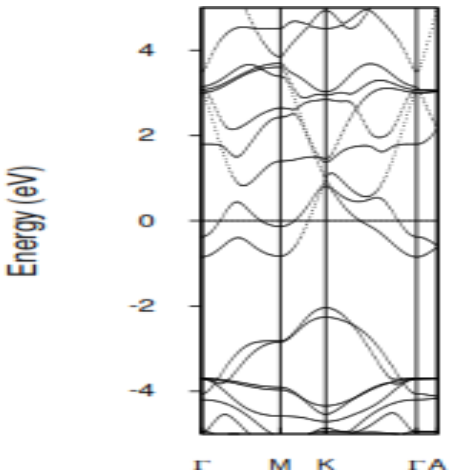

Fig. 15 Bands of WZ in $Mg_{0.5}0Bi_{0.5}0$

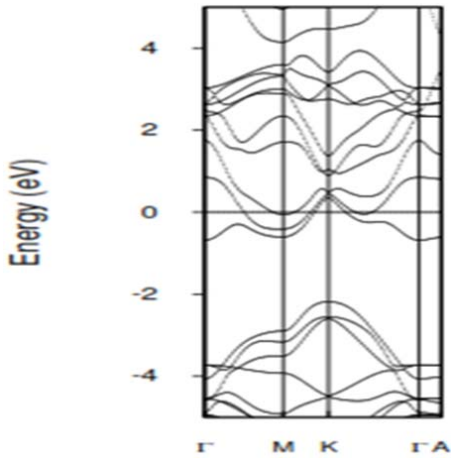

Fig. 16 Bands of WZ in $Mg_{0.25}Bi_{0.75}O$

In Figs. 17-24, it can be observed that the total and partial DOS show the electronic contribution of the above bands. In general, in all these figures the zero energy has been placed at the NF. This level divides the electronic DOS contribution of valence and conduction.

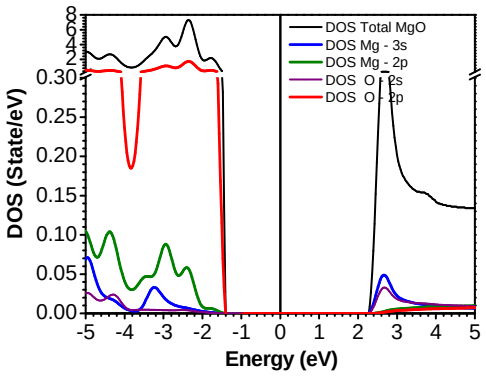

Fig. 17 Total and partial density of state (DOS) for the NaCl in MgO

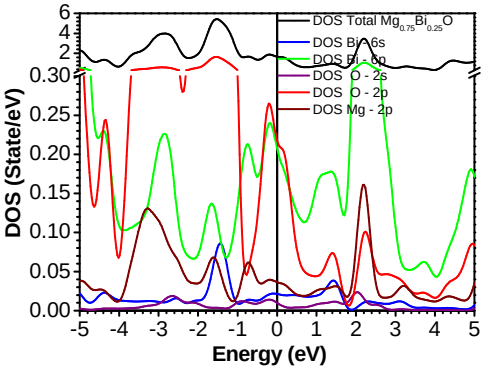

Fig. 18 Total and partial density of state (DOS) for the NaCl in $Mg_{0.75}Bi_{0.25}O$

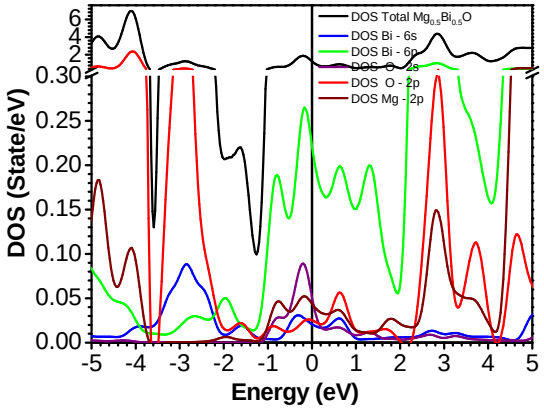

Fig. 19 Total and partial density of state (DOS) for the NaCl in $Mg_{0.5}Bi_{0.5}O$

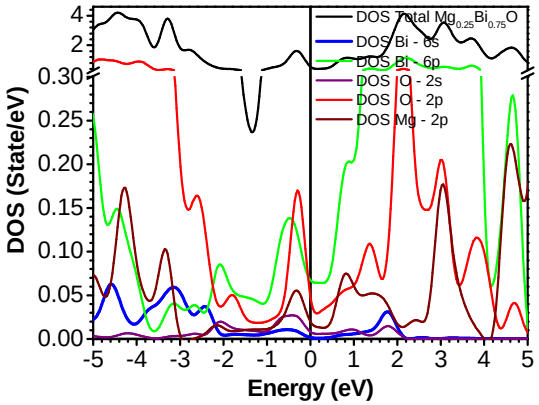

Fig. 20 Total and partial density of state (DOS) for the NaCl in $Mg_{0.25}Bi_{0.75}O$

A. Electronic Properties for the $Mg_{1-x}Bi_xO$ in the NaCl Phase

Figs. 9-12 show the band structure and Figs. 17-20 the DOS for the concentrations of Bi. The dispersion relations show that for MgO there is a large energy gap of ~4 eV with a direct gap at the Γ point, while the remaining three concentrations show metallic behavior. In Fig. 17 to Fig. 20, the electronic contribution around the NF is mainly due to the *p* orbitals of O and Bi, and it can be seen that for 25% it is greater than for 75%. Also, there are small contributions from the *s* orbitals of Mg and Bi, and the *p* orbital of Magnesiun.

B. Electronic Properties for Mg_{1-x} Bi_xO in the WZ Phase

Figs. 13-16 show the bands in the WZ phase. It can be seen that the same as in the NaCl phase of MgO there is also a large gap at point Γ of ~ 3 eV, and in the remaining three concentrations this compound exhibits metallic behavior due to the presence of a union of the overlapped bands around the NF. It can also be seen that there is a very large gap at point K for 50% and 75% Bi. Figs. 21-24 show the partial and total DOS, where for MgO the energy gap can be seen, and for the other concentrations the largest electronic contributions are the *p* orbitals of Bi with small contributions from the *s* and *p*

orbitals of the Mg and the O.

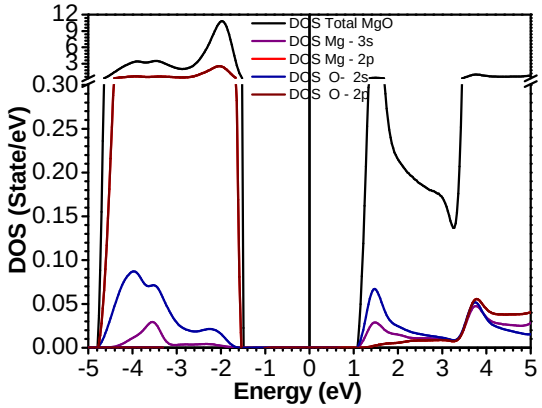

Fig. 21 Total and partial density of state (DOS) for the WZ in MgO

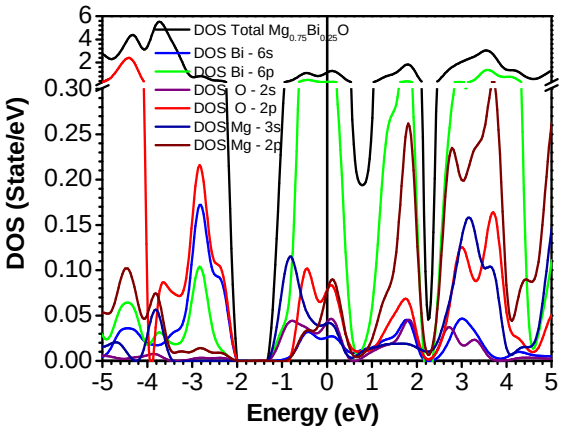

Fig. 22 Total and partial density of state (DOS) for the WZ in $Mg_{0.75}Bi_{0.25}O$

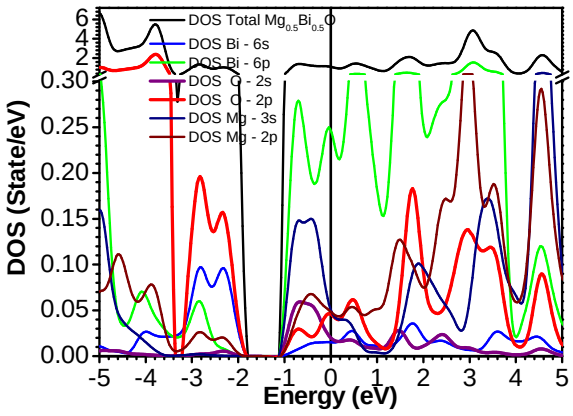

Fig. 23 Total and partial density of state (DOS) for the WZ in $Mg_{0.5}Bi_{0.5}O$

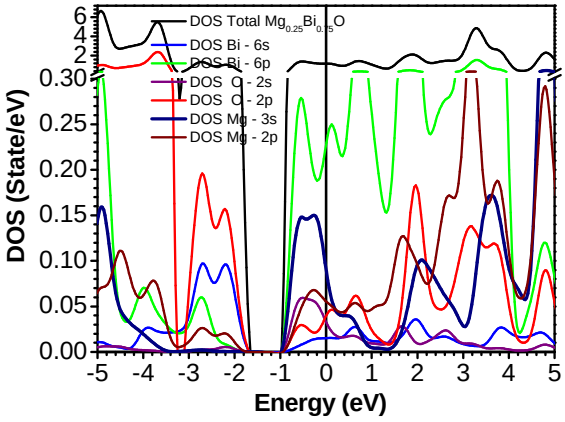

Fig. 24 Total and partial density of state (DOS) for the WZ in $Mg_{0.25}Bi_{0.75}O$

V. Conclusion

Calculations of structural and electronic properties of $Mg_{1-x}Bi_xO$ were carried out by means of DFT using the Wu-Cohen GGA approximation. Our calculations predict that for Bi concentrations greater than ~71%, the WZ structure is more favorable than the NaCl one and that for $x = 0$ (pure MgO), $x = 0.25$ and $x = 0.50$ of Bi concentration the NaCl structure is more favorable than the WZ one. For $x = 0.75$ of Bi, a transition from wurtzite towards NaCl is possible, when the pressure is about 22 GPa. Also It has been observed the crystal lattice constant closely follows Vegard's law, that the bulk modulus and the cohesion energy decrease with the concentration x of Bi. It was determined that for MgO in all three phases two main regions can be observed. One corresponds to an energy gap of ~ 3 eV and the other above ~ -1 eV mainly made up of the p orbitals of O, while for the other three concentrations (¼, ½ and ¾ x bismuth) the behavior of the $Mg_{1-x}Bi_xO$ compound is metallic.

References

[1] G. Patricia Abdel Rahim, J. Arbey Rodriguez y M.G. Moreno Armenta, "Study ab-initio of the stability of the structural and electronic properties of $Bi_{1-x}Mg_xO$," ITECKNE, vol. 11, 2014, pp. 84 – 92.

[2] B. Amrani, R. Ahmed, F. El. Haj. Hassan, "Structural, electronic and thermodynamic properties of wide band gap $Mg_xZn_{1-x}O$ alloy," Computational Materials Science, vol.40, 2007, pp. 66-72.

[3] G. Murtanza, I. Ahmad, B. Amin, A. Afaq, F. Ghafoor, A. Benamrani, "Linear and non-linear optical response of $Mg_xZn_{1-x}O$: A Density Functional study," Physica B: Condensed Matter, vol. 406, 2011, pp. 2632- 2636.

[4] G. Zhao, H. F. Mu, X. M. Tan, D. H. Wang, C. L. Yang, "Structural and dynamical properties of $MgSiO_3$ melt over the pressure range 200-500 GPa: Ab initio molecular dynamics," Journal of Non-Crystalline Solids, vol. 385, 2014, pp. 169-174.

[5] Ph. Hofmann, "The surfaces of bismuth: Structural and electronic properties," Science Direct, vol. 81, 2006, pp. 191-245.

[6] G. Patricia Abdel Rahim, J. Arbey Rodriguez y M.G. Moreno Armenta, "The influence of pressure on the structural and electronic properties of Bi"

[7] G. Patricia Abdel Rahim, J. Arbey Rodriguez y M.G. Moreno Armenta, "Transiciones de fases y gap directo – indirecto inducidas por presión en MgO: Estudio mediante DFT" Rev. Cub. Fis. 31 No 1 E, E22 (2014).

[8] P. Giannozzi, S. Baroni, N. Bonini, M. Calandra, R. Car, C. Cavazzoni, D. Ceresoli, G. L. Chiarotti, M. Cococcioni, I. Dabo, A. D. Corso, S. de

Gironcoli, S. Fabris, G. Fratesi, R. Gebauer, U. Gerstmann, C. Gougoussis, A. Kokalj, M. Lazzeri, L. Martin-Samos, N. Marzari, F. Mauri, R. Mazzarello, S. Paolini, A. Pasquarello, L. Paulatto, C. Sbraccia, S. Scandolo, G. Sclauzero, A.P. Seitsonen, A. Smogunov, P. Umari, and R. M. Wentzcovitvh, "Quantum Espresso: a modular and ftware proyect for quantum simulations of materials" J. Phys. Condens. Matter, 21, 2009, p. 395502. Rev. Acad. Colomb. Cienc., 37 (1), 2013, pp 47-51.

[9] J. Perdew, K. Burke, M. Ernzerhof, Phys. Rev. Lett.77, 1996, p. 3865.

[10] K. Laasonen, A. Pasquarello, R. Car, C. Lee, D. Vanderbilt, "Car-Parrinello molecular dynamics with Vanderbilt ultrasoft pseudo-potentials," Physical Review B, vol. 47, 1993, pp. 10142-10153.

[11] H. J. Monkhorst, J. D. Pack, "Special points for Brillouin-zone integrations," Phys. Rev. B, vol. 13, 1976, pp. 5188-5192.

[12] M. Methfessel, A.T. Paxon, Phys. Rev. B., 40 (1989), p. 3616.

[13] F. D. Murnaghan, Proc. Natl. Acad. Sci., USA 30:244, 1994, 49.